Triple-Band Electrochromic Switching among Visible (400–750 nm), NearIR-I (750–1000 nm), and NearIR-II (1000–1600 nm) Regions with Triple-Redox-Active Metallosupramolecular Polymers

*Dines Chandra Santra, Sanjoy Mondal, Banchhanidhi Prusti and Masayoshi Higuchi**

Electronic Functional Macromolecules Group, National Institute for Materials Science (NIMS), 1-1 Namiki, Tsukuba 305-0044, Japan, E-mail: HIGUCHI.Masayoshi@nims.go.jp

KEYWORDS: VIS–NIR, dual-band electrochromic, multicolor, metallosupramolecular polymer, triple redox, durability, smart windows

ABSTRACT: Selective electrochromic (EC) switching in the wide range from visible (VIS) to near-infra-red (NIR) wavelengths was achieved using novel triple-redox-active metallosupramolecular polymers (MSPs), synthesized by 1:1 complexation of a transition metal salt and a bisterpyridine ligand containing a tetraphenylbenzidine (TPB) moiety. By tuning an oxidation potential in the range between 0 V and 1.2 V vs. Ag/Ag^{+},

the MSPs (**polyFeL$_{TPB}$** and **polyRuL$_{TPB}$**) were capable of selective and reversible triple-band EC modulation in the visible (400–750 nm), NIR-I (750–1000 nm), and NIR-II (1000–1600 nm) regions. Interestingly, the polymers exhibited excellent EC properties with remarkably high optical contrast (98%), high coloration efficiency (CE) (851 cm^2/C), and fast switching even in the NIR region. A made-to-order quasi-solid-state EC device exhibited exceptionally long cycle stability (>7000 cycles) from the visible to the NIR region at an incredibly low operational voltage (1.2 V). These two ECDs demonstrated that a significant amount of solar irradiance (about 33–36%) shielding in the NIR band at 750–1670 nm while allowing 46–53% of VIS transparency under low voltage. At dark mode at 0.8 V, they exhibit 59–63% of VIS and 45–47 % NIR blocking. Under full oxidation, ECDs screen 51–60% VIS and 36–41% NIR while using very small electrical energy (about 1.7–13.5 mJ cm^{-2}). These findings signify a significant advancement in the design of large scalable dual-band EC devices.

1. INTRODUCTION

Lighting, heating, and air conditioning in buildings utilize between ~40 percent of the world's primary energy.[1, 2] Based on the weather and user preferences, a smart window can control the transmission of visible (VIS) and near infrared (NIR) light to lower the overall amount of solar light passing through the window.[3-5] As the NIR area makes up roughly half of the total solar radiation, the ability to modulate NIR transmittance dynamically and selectively through the windows has a significant impact on the heating and cooling, energy consumption.[6] A promising method has been provided using electrochromic (EC) materials, which intelligently adapt to potential bias as transmittance changes. EC materials, which may modify transmittance or color change

by applied voltages, can be used in a wide range of user-friendly applications, such as screens, rear-view mirrors for cars, e-papers, and EC e-skins.[7-11] EC-based smart polymers are excellent candidates for independently controlling the transmittance of visible and NIR sunlight entering buildings, automobiles, and aircraft.[12-14] To provide selective, dynamic switching over the transmission of solar radiation, an ideal EC material should have excellent high optical contrast, rapid response time, extended cycle durability, and affordable production cost. A wide range of EC materials, including metal oxides,[13] metal complexes,[15] small organic molecules,[16] conjugated electroactive polymers,[17] and metal–organic frameworks,[18-20] have been employed for ultraviolet (UV)–VIS–NIR applications. Recently, more effort has been extended towards discovering new EC materials that exhibit UV–VIS–NIR absorbing properties. There are many ECD studies for multicolor VIS–NIR control, which struggle with the preliminary prototype concept, thereby delaying their commercialization.[21, 22] Thus, transition metal oxides,[9, 23, 24] viologen,[25] conducting polymers,[26-28] and other inorganic and organic materials have been studied as EC materials with great success. Commercial applications of electrochromic smart windows are restricted by high manufacturing costs, unsatisfactory charge capacity, low coloration efficiency, and short-term durability due to limitations in functionality, cost, and robustness.[11, 29] For instance, although organic electrochromic materials make the devices extremely flexible and wearable, their poor light-exposure durability hinders their practical use.[29, 30] Inorganic electrochromic devices made of transition metal oxides exhibit enhanced performance through structural and chemical improvements, but face material degradation from ion insertion.[31, 32] Many recently conjugated organic polymers and MSPs exhibit color versatility.[33-39] EC MSPs are anticipated to have certain advantages

over inorganic or organic materials, such as a long-life cycle, coloration efficiency (CE), high ΔT, and fast switching ability. Thus, they are at the forefront of real-world applications and commercialization. Among them, only a few EC materials exhibit unlimited color versatility.[40-42] Unfortunately, a very low number of reported EC materials are applicable for absorbance in selectively visible or NIR light.[9, 43, 44] The preparation of suitable ligand materials that can form complex to redox-active metal ions and translate them into selective, controllable, and reversible EC action is one of the most interesting and challenging research topics on EC materials.

Herein, we report a new strategy to triple-band electrochromic switching among visible (400–750 nm), nearIR-I (750–1000 nm), and nearIR-II (1000–1600 nm) Regions. We synthesized 4,4'-bis-(2,2:6,2-terpyridinyl)-tetraphenylbenzidine **(L$_{TPB}$)** as a new redox-active ligand (Scheme 1a). New MSPs (**polyFeL$_{TPB}$** and **polyRuL$_{TPB}$**), prepared by the complexation of the ligand with Fe(II) or Ru(II) ions, our new ligand, have three redox-active sites (two nitrogen atoms and the metal ion) (Scheme 1b). This time we have chosen Fe(II)/Ru(II) as promising metal ions to form a high molecular weight polymer this time, because two terpyridine moieties of **L$_{TPB}$** bind with the metal ions strongly. By altering the applied voltages, these two MSPs can produce a homogeneous film surface and a VIS–NIR active film that is multicolored. The presence of TBP units in the ligand not only preserves the physical properties, such as high thermal stability and increase in solubility but also provides an electroactive unit within the ligand structure to achieve essay processing and unique applications.[45]. By adjusting the applied redox potential, we hypothesized that the resulting MSP film would be

multicolored with rapid and reversible EC activity at VIS (400–780 nm) and NIR (750–1600 nm) wavelengths.

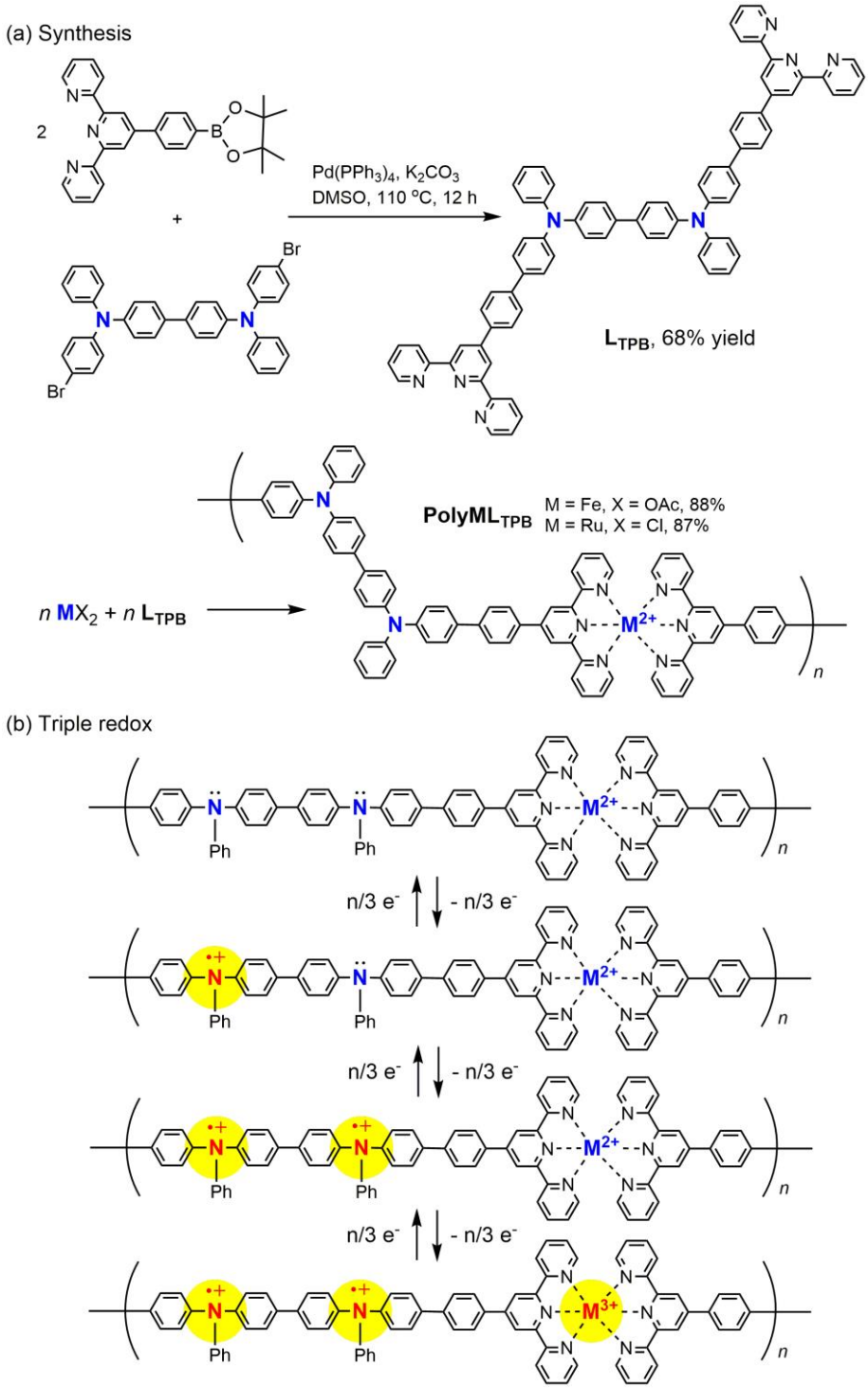

Scheme 1. (a) Synthesis of **L**$_{TPB}$ and **polyML**$_{TPB}$ (M: Fe(II) or Ru(II)) and (b) the triple redox system at the two nitrogen atoms and the metal.

2. RESULT AND DISCUSION

Two terpyridine (Tpy) arms based on an electroactive ligand were synthesized for MSP formation. **TPB** was judicially selected as a redox-active chromophore linked to Tpy for extended MSP formation with different metal ions through complexation. To create the **L$_{TPB}$** ligand, a Pd(0) catalyst was used in a straightforward Suzuki-coupling process that resulted in the high yield of a light green-yellow solid that could be characterized using various methods, including proton nuclear magnetic resonance (^{1}H-NMR), ^{13}C-NMR, and electrospray ionization (ESI)-mass spectrometry (Figures S1–S3, supporting information (SI)). To understand the polymer formation, we investigated the complexation behavior of **L$_{TPB}$** with Fe(II) ions in a UV–VIS study (Figure 1a). The colorless solution of the **L$_{TPB}$** ligand exhibited two absorption peaks for the π–π* and n–π* transitions at 282 and 372 nm, respectively. However, when Fe(II) ions were added to **L$_{TPB}$**, the color of the solution abruptly changed from colorless to red wine. A new peak at 576 nm was observed, resulting from a metal-to-ligand charge transfer (MLCT) transition. When the Fe(II) ion and **L$_{TPB}$** molar ratio was 1:1 in the solution mixture, the peak at 576 nm was saturated. This result indicated that Fe(II) ions were present and hexacoordinately bound with **L$_{TPB}$** at a 1:1 molar ratio.[46-48]

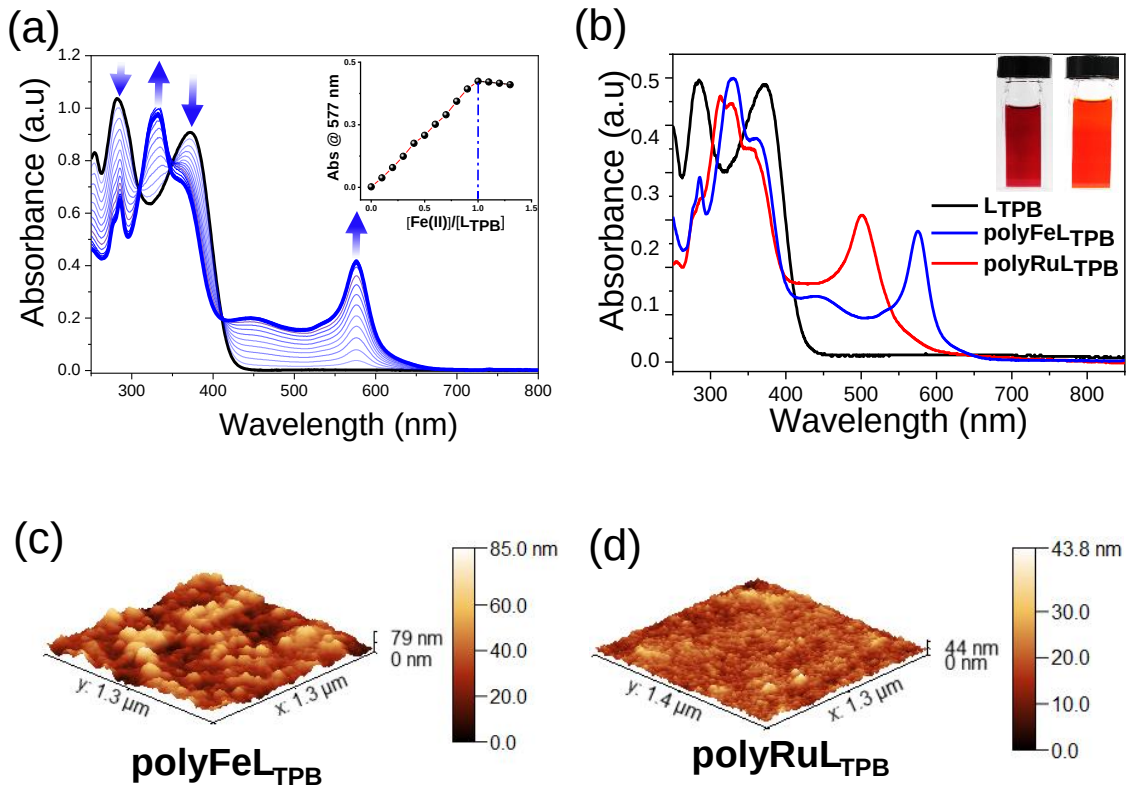

Figure 1. (a) UV–VIS spectral changes during the stepwise complexometric titration of **L**$_{TPB}$ with Fe(II) ions in MeOH/$CHCl_3$ (1:1) at room temperature. The inset shows the absorption change at 577 nm as a function of the [Fe(II)]/[L_{TPB}] ratio. (b) UV–VIS spectra of **L**$_{TPB}$ in $CHCl_3$ and **polyFeL**$_{TPB}$ and **polyRuL**$_{TPB}$ in methanol (inset: images of the methanolic polymer solution). (c) **PolyFeL**$_{TPB}$ and (d) **polyRuL**$_{TPB}$ films and the atomic force microscopy images of their surfaces.

Based on the aforementioned titration result, we prepared Fe(II)- and Ru(II)-based MSPs in acetic acid/ethylene glycol media, respectively, with ~ 90% yield. The complete synthetic technique and purification methods are described in the experimental section. The characteristic UV–VIS study for **L**$_{TPB}$ and both polymers (**polyFeL**$_{TPB}$ and

poly RuL$_{TPB}$) are shown in Figure 1b. **L$_{TPB}$** formed a colorless solution and exhibited peaks for the π–π* transition at 282 and 370 nm.[47, 49, 50]

By complexing **L$_{TPB}$** with Fe(II) and Ru(II) metal ions, a significant absorption band was observed at 571 nm for **polyFeL$_{TPB}$** and 500 nm for **polyRuL$_{TPB}$**, respectively, as indicated by the red wine and orange solutions in methanol (inset, Figure 1b). These two strong peaks in the visible region originated from MLCT transitions from the metal (Fe/Ru) to **L$_{TPB}$**. Another weak broad signal was observed at 440 nm for both polymers, indicating that the polymers were twisted in the configuration in the polymer chain.

In comparison with the free ligand, ^{1}H NMR confirmed the complexometric association between **L$_{TPB}$** and the metal ions [Fe(II)/Ru(II)] within the polymer chains. (Figure S4, SI). In the ^{1}H-NMR analysis, the downshifted and broad peak between **L$_{TPB}$** and the polymers (**polyFeL$_{TPB}$** and **polyRuL$_{TPB}$**) implied high-molecular-weight polymer chain formation, which shortened the relaxation time. Additionally, the NMR study suggested that the large shifts of all the aromatic protons to the low-field region, compared with the free ligand, **L$_{TPB}$**, after polymer formation by complexation between **L$_{TPB}$** and the metal ions [Fe(II)/Ru(II)], occurred without any side reaction because of the high coordination ability of the two Tpy arms of **L$_{TPB}$**. To confirm the molecular weight of both polymers, we measured the average molecular weight (M_w) using the size exclusion chromatography-viscometry-right angle light scattering (SEC-VISC-RALS) method with polyethylene oxide (PEO) as a standard (Figure S5, SI). The study obtained $M_w = 3.3 \times 10^5$ and 2.7×10^4 Da for **polyFeL$_{TPB}$** and **polyRuL$_{TPB}$** in methanol, respectively. Thermogravimetric analysis (TGA) was conducted at temperatures between 25 and 550°C in an N_2-saturated atmosphere. Figure S6a (SI) shows that when the temperature rises, both polymers steadily decomplexate. However, it is expected that

the polymers are fairly stable for use in smart window applications. The thermal stability among **L$_{TPB}$**, **polyFeL$_{TPB}$**, and **polyRuL$_{TPB}$** showed that free ligands decompose at higher temperatures, compared with both polymers. This result was also analogous to reported MSPs with Tpy as the complexing ligand.[47] The powder X–ray diffraction(XRD) study confirmed that **polyFeL$_{TPB}$**, and **polyRuL$_{TPB}$** both are amorphous in nature (Figure S6b, SI). Atomic force microscopy (AFM) was employed to examine the surface morphology of the polymer films, as illustrated in Figures 1c and d. The topology of both polymer films revealed a roughly flat surface with homogenously assembled spherical polymers with a diameter of nanometer size. Additionally, AFM showed that **polyRuL$_{TPB}$** had a lower roughness of 1.36 nm, compared with that of 3.49 nm for **polyFeL$_{TPB}$**.

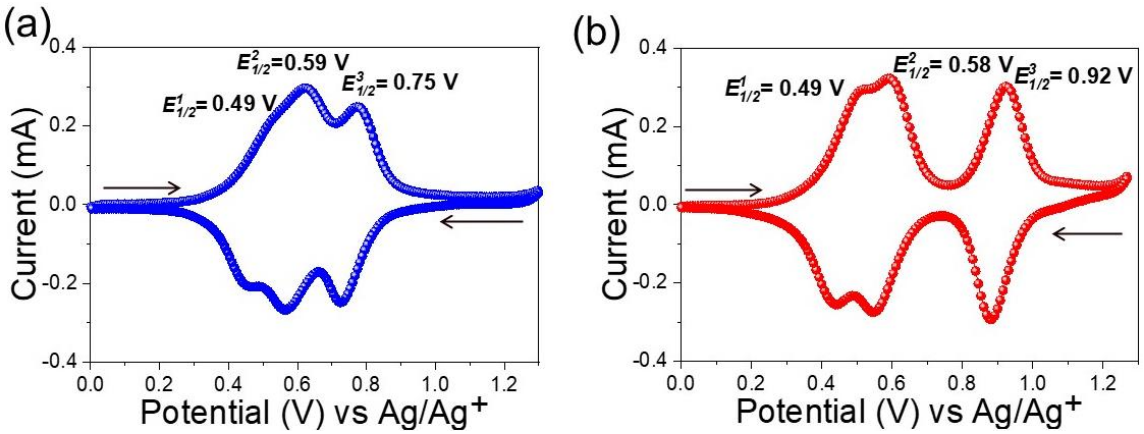

Figure 2. Cyclic voltammogram of (a) **polyFeL$_{TPB}$** and (b) **polyRuL$_{TPB}$** in an acetonitrile solution containing 0.1 M $LiClO_4$ at a scan rate of 50 mV/s.

Indium tin oxide (ITO) glass was used as the working electrode (WE), Pt wire served as the counter electrode (CE), Ag/Ag^+ saturated with 0.1 M tetrabutylammonium phosphate (TBAP) + 0.01 M $AgNO_3$ served as the reference electrode, and 0.1 M $LiClO_4$/acetonitrile served as the supporting electrolyte. Thus, we investigated the electrochemical properties of both polymer films in a conventional three-electrode system. Cyclic voltammetry (CV) showed that both polymer films exhibited reversible redox activity (Figure 2). Three pairs of reversible redox peaks were visible in the anodic scan of both polymers between 0 and 1.3 V (vs. Ag/Ag^+). Figure 2 a shows three redox peaks $E_{1/2}$ at 0.49, 0.59, and 0.75 V for **polyFeL$_{TPB}$** and 0.49, 0.58, and 0.92 V for **polyRuL$_{TPB}$** (Figure 2 b). The first redox peak $E^1_{1/2}$ for **polyFeL$_{TPB}$** was observed at 0.49, formed by the radical cation of triphenylamine ($N/N^{\bullet+}$), whereas the second peak, $E^2_{1/2}$ at 0.59, was due to the formation of a dication ($N^{2\bullet+}$) in the TBP unit.[51-54] The third redox peak $E^3_{1/2}$ for **polyFeL$_{TPB}$** was due to the oxidation of the metal centers [Fe(II)→ Fe(III)] at 0.75 V.[47] When the metal center was changed to the Ru(II) ion in **polyRuL$_{TPB}$**, three separable reversible peaks were observed. Figure 2b shows the redox peak $E^1_{1/2}$ at ~ 0.49 V (vs. Ag/Ag^+) for the formation radical cation of triphenylamine ($N/N^{\bullet+}$) of the **TPB**. The potential $E^2_{1/2}$ at ~ 0.58 V was due to the formation of a dication ($N^{2\bullet+}$) of the **TPB** unit. Eventually, the [Ru(II)→Ru(III)] oxidation and completion of all the oxidation centers within the polymer chain occurred $E^3_{1/2}$ at 0.90 V (vs. Ag/Ag^+). Figure S7 (SI) shows that these two polymers linearly increased with the square root of the scan speed, suggesting that diffusion control between the film surface and electrolytes was the mechanism causing the redox change.

The net charge ratio for both polymers was ~ 1.0, indicating that the polymers would be highly stably redox-active for long-time switching (Figure S8, SI).

Spectroelectrochemical analysis of polyFeL$_{TPB}$ and polyRuL$_{TPB}$ films

To understand the electronic structures and optical properties of polymer films, we performed in situ spectroelectrochemical experiments in a three-electrode system coupled with a UV–VIS–NIR spectrophotometer. In a three-electrode system with a 0.1 M $LiClO_4/CH_3CN$ electrolyte, Ag/Ag^+ served as the reference electrode, polymer-coated ITO glass served as the WE, and Pt spring served as the CE. As shown in Figure 3a, the brown (L* = 43.9, a* = 28.5, b* = 19.7) **polyFeL$_{TPB}$** exhibited a robust absorption band that was visible at 577 nm, corresponding to MLCT electronic transitions between Fe(II) and **L$_{TPB}$**. The TBP unit in **polyFeL$_{TPB}$** was gradually oxidized at 0.55 V (vs. Ag/Ag^+) to radical cations, as shown by the appearance of a new band at 503 nm and a broad intense band in the NIR region between 1240 and 1600 nm resulting from a typical triarylamine radical-cation species (Figure S9a, SI) with a color change from brown to brick red (L* = 32.8, a* = 37.2, b* = 13.1). This broad absorption band was centered around 1240 nm in the NIR region because of the characteristic IVCT excitation of the $N \rightarrow N^{\bullet+}$ center of the TPB moiety in the polymer skeleton[47, 55-57] (Figure S9a, SI). The electrogenerated MV system was classified as a symmetrical delocalized class III structure according to Robin and Day.[58] After applying an anodic potential of ~ 0.7 V, a new broad band centered around 800 nm appeared. Consequently, the two absorption bands for the radical cation gradually decreased (Figure S9b, SI). We observed that the NIR absorption disappeared owing to further oxidation from the radical cation species to the formation of dications in the **TPB** segments associated with

a color change of the polymer film from brick red to black (L* = 24.4, a* = 8.3, b* = −18.2). As the positive potential increased to ~ 1.0 V, the absorption bands at 577 nm from an MLCT gradually decreased, but the broad band positioned around 800 nm remained unaltered (Figure S9c, SI). The unique peak shifts at 577 nm were due to the reversible oxidation of the metal core [Fe(II) → Fe(III)]][47] in conjunction with the dication states of the TPB moiety inside the polymer chain. The **polyFeL$_{TPB}$** film changed its color from black to greenish-blue (L* = 33.7, a*= −19.2, b* = −4.8) because of this transition. The overall transmittance changes between 400 and 1660 nm at different potentials of **polyFeL$_{TPB}$** are presented in Figure S9d in SI.

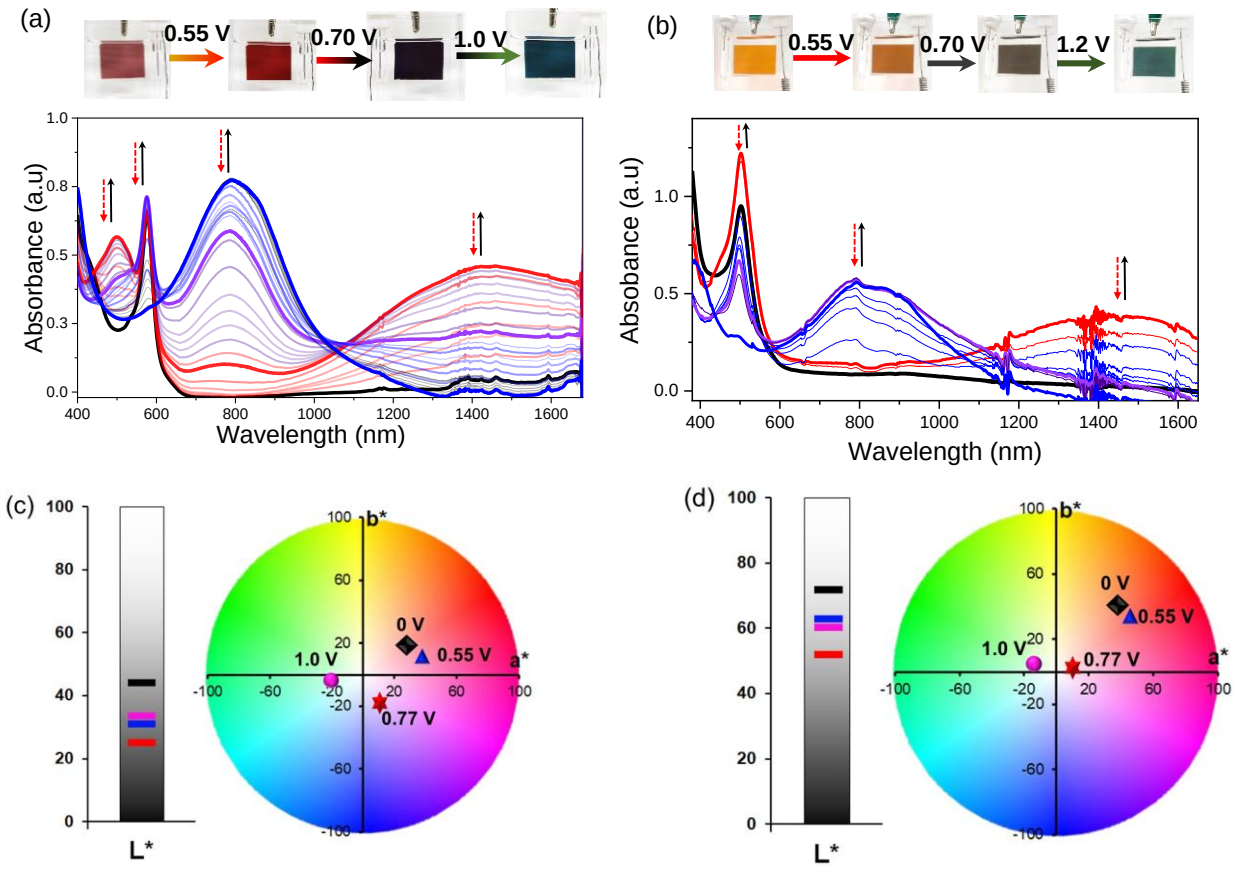

Figure 3. UV–VIS–NIR spectroelectrochemistry in a 0.1 M $LiClO_4$ electrolyte. (a) **PolyFeL$_{TPB}$** film at applied potentials from 0 to 1.05 V. (b) **PolyRuL$_{TPB}$** film at applied

potentials from 0 to 1.25 V. CIE 1976 color diagram of the (c) **polyFeL$_{TPB}$** and (d) **polyRuL$_{TPB}$** films in different colors at different potentials.

Similar results observed for the **polyRuL$_{TPB}$** film (Figure 3b) showed a reversible color change upon step-wise oxidation. In the neutral state, an orange film (L* = 71.4, a* = 38.6, b* = 41.4) exhibited an MLCT band at 500 nm. Upon applying ~ 0.52 V (vs. Ag/Ag^{+}), a new broad absorbance band was observed within ~ 1200–1600 nm, and the intensity of the ~ 503-nm band simultaneously increased (Figure S10a, SI). During these electrochemical modifications, the hue of the film changed from orange to orange-red (L* =61.9, a* =42.0, and b* = 36.0). The **TBP** moiety in the polymer chain formed a monoradical cation, which caused this event. A further increase in the potential to 0.7 V caused two absorption bands for the radical cations (503 nm and the broad band within the range of 1200–1600 nm) to gradually decrease (Figure S10b, SI), and the color changed from orange-red to blackish (L* = 51.0, a* = 11.5, b* = 1.6). However, the MLCT band was unaffected at this applied potential. The oxidation of [Ru(II)→ Ru(III)][59] and the existence of the dication state in the polymer backbone caused the intensities of the MLCT absorption peaks at 500 and 800 nm to gradually diminish as the applied potential increased at 1.2 V (Figure S10c, SI), and the color changed from blackish to greenish-blue (L* = 59.6, a* = −15.8, b* = 2.8). Therefore, both polymers exhibited multiple colors at different potentials and tuned the absorption regions visible to NIR. The Commission Internationale de l'Éclairage (CIE) (1976) chromaticity diagrams for both polymers were calculated at different potentials[60] and are shown in Figures S11 and S12 and Table S1. The overall transmittance changes between 400 and 1660 nm at different potentials of **polyRuL$_{TPB}$** are presented in Figure S10d in SI.

To examine the EC performance of the polymer films, both spray-casted polymers were deposited on ITO-coated glass slides, and a commercial UV–VIS cuvette was used. Figure 4a shows the optical switching and EC stability of **polyFeL$_{TPB}$** investigated at three voltage intervals of 0–0.55, 0.55–0.70, and 0.70–1.0 V separately in a 0.1 M $LiClO_4$ electrolyte solution. **PolyFeL$_{TPB}$** exhibited an optical contrast (ΔT) of ~ 28%, 14%, and 98% at 503, 577, and 800 nm, respectively. As shown in Figure 4a, optical change (ΔT-t) via EC switching was observed at 503, 577, and 800 nm and repeated without altering the optical contrast for several cycles. The response time was calculated at 95% of the full switching (bleaching (t_b) and coloration time (t_c)) monitoring at three transmittance peaks (503, 577, and 800 nm), and it was between 0.3 and 2.2 for 503 nm, 1.1 and 3.3 s for 577 nm, and 0.8 and 1.7 s for 800 nm. This suggested a very good stable and rather fast, responsive EC polymeric film. In addition, the optical contrast and CE of **polyFeL$_{TPB}$** were investigated between 0 and 1.0 V. **PolyFeL$_{TPB}$** exhibited optical contrasts of 28%, 14%, and 98% at 503, 577, and 800 nm, respectively, with a CE of 377 cm^2/C at 503 nm, 332 cm^2/C at 577 nm, and 851 cm^2/C at 800 nm. Similarly, for **polyRuL$_{TPB}$**, the optical switching was investigated between three voltage intervals (0–0.55, 0.55–0.70, and 0.70–1.2 V) separately in a three-electrode system using a 0.1 M $LiClO_4$ electrolyte solution. **PolyRuL$_{TPB}$** shows (Figure 4b) the optical contrasts of ~ 5% for monoradical cation formation at 500 nm, ~23% for the oxidation of [Ru(II)→ Ru(II)] at the same wavelength, and ~ 88% at 800 nm. The coloration time was 1.7, 1.3, and 1.4 s at 503, 500, and 800 nm, respectively, whereas the bleached time was only 0.8, 1.2, and 0.9 s at 503, 503, and 900 nm. The calculated CE values were 123 cm^2/C at 503

nm for monoradical formation, 528 cm^2/C at 500 nm for the oxidation of the Ru(II) metal center, and 714 cm^2/C at 800 nm for dication formation. The EC results are summarized in **Table 1**.

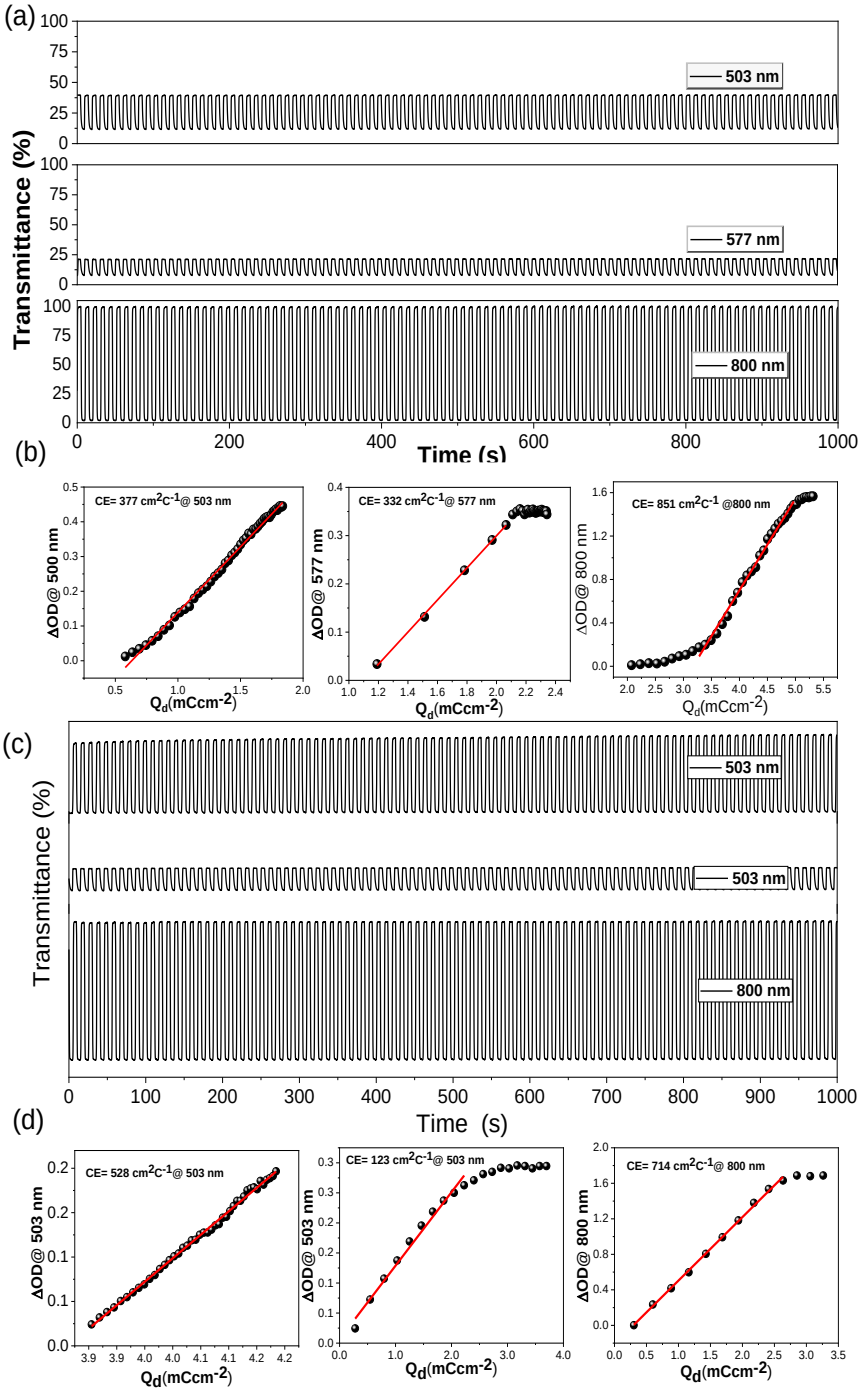

Figure 4. Electrochromic (EC) switching between (a) 0 and 0.55 V centered at 503 nm, 0.55 and 0.77 V centered at 800 nm, and 0.77 and 1.0 V centered at 577 nm (vs. Ag/Ag^{+}) of the **polyFeL$_{TPB}$** thin film on the ITO-coated glass substrate (coated area: 1.1

× 1.2 cm^2) in 0.1 M $LiClO_4/CH_3CN$ with a cycle time of 5s. (b) Optical density (ΔOD) versus charge density (Q_d) of **polyFeL$_{TPB}$** at a given wavelength. (c) EC switching between 0 and 0.55 V at 503 nm, 0.55 and 0.77 V at 800 nm, and 0.77 and 1.2 V at 500 nm (vs Ag/Ag^+) of the **polyRuL$_{TPB}$** thin film on the ITO-coated glass substrate (active area: 1.1 × 1.2 cm^2). (d) Optical density (ΔOD) versus charge density (Q_d) at a given wavelength in 0.1 M $LiClO_4/CH_3CN$ with a cycle time of 5s.

Table 1: Summarized electrochromic results of **polyFeL$_{TPB}$** and **polyRuL$_{TPB}$**.

Polymer	λ_{max} (nm)	Potential (V) vs. Ag/Ag^+	Optical contrast (ΔT, %)	Response time (s) [t_c and t_b]	Coloration efficiency (cm^2/C)
polyFeL$_{TPB}$	503	0.55	28	2.2/0.3	377
	577	1.0	14	3.3/1.1	332
	800	0.77	98	1.7/0.8	851
polyRuL$_{TPB}$	503	0.55	5	1.7/0.8	123
	500	1.2	23	1.3/1.2	528
	800	0.77	88	1.4/0.9	714

Fabrication and electrochromic properties of all-solid-state ECDs

We fabricated a 2.5 × 2.5 cm^2 all-solid-state ECD using **polyFeL$_{TPB}$** or **polyRuL$_{TPB}$** coated on ITO as the WE, a NiCHF-coated ITO glass as the CE, and a mixture of poly(methyl methacrylate) (PMMA) and $LiClO_4$ as a semisolid electrolyte (Figure 5). The complementary chromic combination of cathodically coloring polymer and anodically coloring NiHCF. It's reported that NiHCF showed the highest electrochemical stability against the repeated color changes in device state.[61] Details of the device fabrication methods are described in the experimental section. The two ECD

electrodes of **polyFeL$_{TPB}$** exhibited a reversible multicolor change from brown→red-brown→black→greenish color (Figure 5b) in a potential range of 0–1.0 V. The CV curve of the device exhibited an excellent reversible redox propert between 0 to 1.5 V and the maximum optical modulation at 800 nm (Figure S13a,b, SI). At 800 nm, the optical contrast was 86% during the EC changes. At 800 nm, the persistence of EC alterations was investigated, and it was shown that 85% of the EC activity remained after more than 7000 cycles (Figure 5c).

Similarly, an ECD with a **polyRuL$_{TPB}$** film exhibited multiple colors from orange→red-orange→brown-black→greenish when the electrical bias was slowly increased from 0 to 1.2 V. **polyRuL$_{TPB}$** device's showed a maximum optical modulation at 800 nm and CV curve exhibited excellent reversible redox property between 0 and 1.5 V (Figure S13c,d, SI). The ECD exhibited a maximum optical contrast of 74% at 800 nm (Figure 5d). During continuous cyclic switching in this NIR region, the device demonstrated stable EC activity and maintained almost 80% of its initial activity after 7000 cycles. Additionally, as demonstrated in Figures 5c and 5d, both ECDs confirm outstanding cyclic stability. Due to the higher voltage needed for ECD of **polyRuL$_{TPB}$**, our constructed ECD of **polyRuL$_{TPB}$** exhibits slightly less stability compared to ECD of **polyFeL$_{TPB}$** after 7000 cycles at ambient temperature[39, 62, 63].

Table 3. EC properties of **polyFeL$_{TPB}$** and **polyRuL$_{TPB}$**.

ECD	λ_{max} (nm)	T_b (%)	T_c (%)	ΔT (%)	switching times(t_c/t_b) (s)	CE (cm^2/C)

PolyFeL$_{TPB}$	800	90.9	8.6	82.3	1.72/1.06	773
PolyRuL$_{TPB}$	800	90.8	15.3	75.5	2.01/1.1	690.3

By varying the applied voltage, our fabricated ECDs can successfully and independently control both the visible (400-780 nm) and NIR (780-1670 nm) transmittance (Figure S12, SI). A good visible transmittance of 68% is kept in the neutral state of the **PolyFeL$_{TPB}$** ECD (Figure S13a, SI). ECD of **PolyFeL$_{TPB}$** transforms into brick red at 0.6 V and maintains transmittance of 53% at visible region while being able to block 33% of NIR light. The ECD enters the "dark black" state at 0.8 V and blocks 47% of NIR and 63% of VIS light. Greenish color block at 1.0 V in complete oxidation state of ECD accounts for 60% VIS and 41% NIR. Similar to this, **PolyRuL$_{TPB}$** ECD (Figure S13b, SI) maintains transmittance of 100% in the NIR region and 52.2% in the visible portion at neutral state. Device turns reddish brown and maintains 46.3% transmittance while blocking 36.6% NIR at 0.6 V. **PolyRuL$_{TPB}$** ECD can block 45.2% of heat in the NIR range and 58.4% of visible light in a black color state. Finally, at 1.2 V, a blackish green device exhibits 51% and 36.5%, respectively, visible and NIR light block. The calculated solar energy of these polymers can be deployed as energy saving smart windows. Figure pointing out that such outstanding electrochromic performance is undoubtedly better. Our MSP thin-film-based devices provided a smart window that saved energy more effectively overall for future applications.

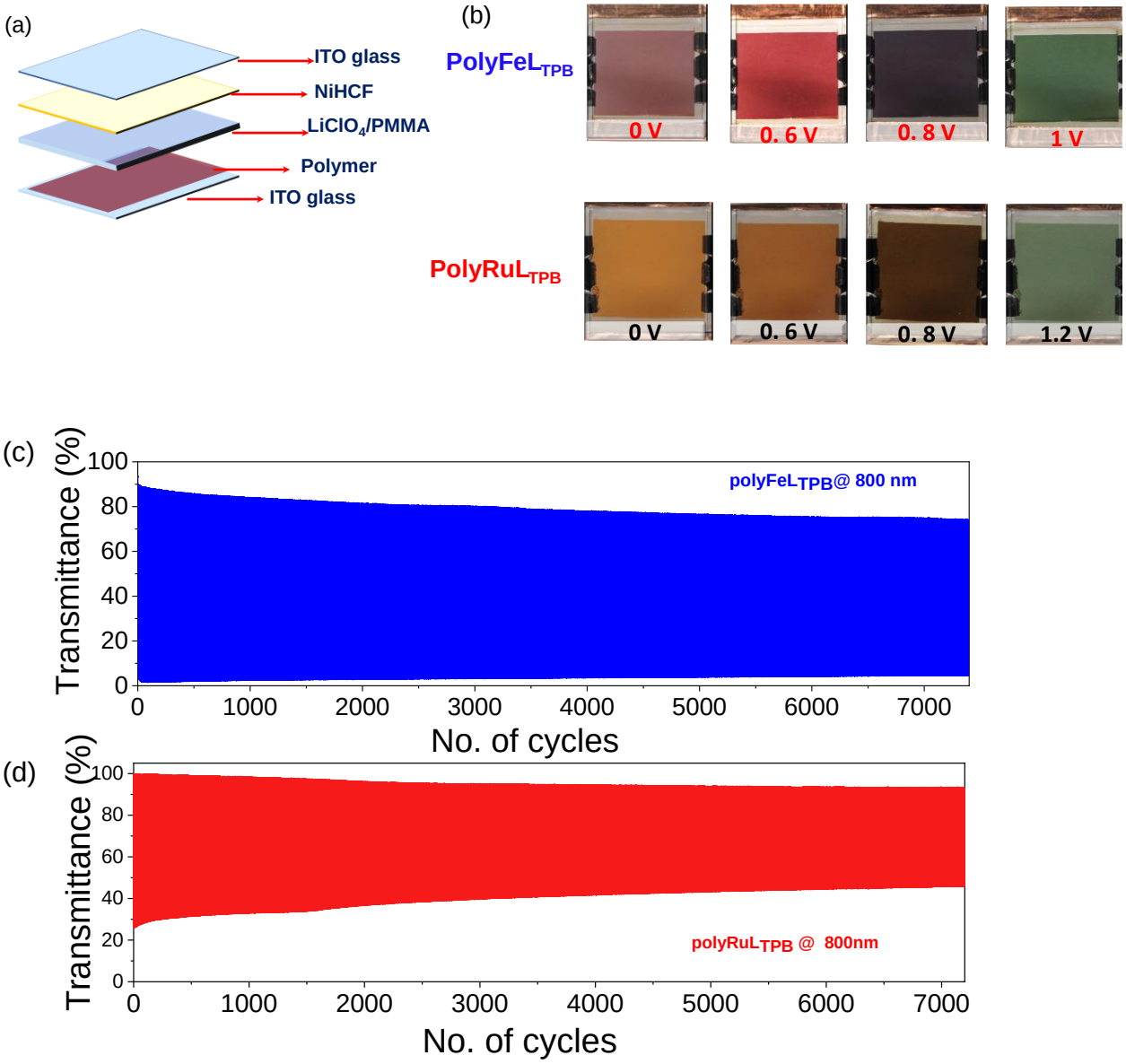

Figure 5 (a) Schematic representation of the fabricated device structure. (b) Color changes of the devices of **polyFeL$_{TBP}$** and **polyRuL$_{TBP}$** films at different potentials. (c) Dynamic transmittance changes of **polyFeL$_{TBP}$** at 800 nm and (d) **polyRuL$_{TBP}$** at 800 nm during the EC cycles (applied voltages between 0 and 1.5 V; each retention time was 2.5 s).

CONCLUSIONS

By complexing **L$_{TPB}$** with either Fe(II) or Ru(II) ions at a ratio of 1:1**,** two MSPs (**polyFeL$_{TPB}$** and **polyRuL$_{TPB}$**) with triple redox states, were achieved. Through several characterization techniques, the chemical structures of the ligand (**L$_{TPB}$**) and polymers were confirmed. At various potentials, both polymers demonstrated three controllable electrochemical redox states. In the step-by-step oxidation of the polymer films, the polymers exhibited exceptional multicolor EC performance with various color changes (brown, red-brown, black, and greenish color for **polyFeL$_{TPB}$**; orange, red-orange, brown, black, and greenish color for **polyRuL$_{TPB}$**). Simultaneously, a strong broad absorption band was observed in the NIR regions in 1200–1600 nm owing to the formation of monoradical cations at a very low potential of ~ 0.55 V *vs*. Ag/Ag^{+}. Another absorption band was observed in the NIR region at 800 nm by applying a potential of ~ 0.77 V *vs*. Ag/Ag^{+} owing to the radical dication formation of the TBP unit. With just one EC layer sandwiched between two conductive electrodes and extremely low working voltages, the synthesized ECD demonstrated multicolor EC activity. Additionally, the proposed ECD demonstrated reversible optical switching when 0/1.5 V was applied and maintained unaltered EC activity in the visible and NIR regions for more than 7000 cycles. Our ECDs can independently control visible (400-780 nm) and NIR (780-1670 nm) transmittance by varying the applied voltage. Both ECD at 0.6 V and transmit 46 to 53% VIS light while blocking 33 to 36% NIR light. ECD becomes "dark black" at 0.8 V, blocking 45 to 47% NIR and 58 to 63% VIS light. Greenish color block at 1.0 to 1.2 V in complete ECD oxidation accounts for 51 to 60% VIS and 36 to 41% NIR. light. Our polymer can be used as energy-saving smart windows for future

applications. The fabricated multi–electrochromic polymers are simple to produce and will have a significant impact on display, smart windows, and e-paper technology.

4. EXPERIMENTAL SECTION

Materials and Tools

PMMA, $LiClO_4$, and acetonitrile were purchased from TCI Co. Ltd and used without further purification. In addition, 4,4′-bis[(4-bromophenyl)phenylamino]biphenyl; $Ru(DMSO)_4Cl_2$; $Pd(PPh_3)_4$; and $Fe(OAc)_2$, were purchased from Sigma-Aldrich. Furthermore, 4'-(4-(4,4,5,5-tetramethyl-1,3,2-dioxaborolan-2-yl)phenyl)-2,2':6',2''-terpyridine (**3**) was synthesized, following a reported method.[46] All the solvents and reagents (analytical grade) were used as received unless otherwise stated. For the structural characterization of the compounds, chloroform-d ($CDCl_3$) was used as the solvent, and a JEOL 400 MHz (JNM-ECZ series) apparatus was used to record the ^1H and ^{13}C NMR spectra. A trapped ion mobility spectrometry time-of-flight spectrometer was used to quantify molecular weight (Bruker, version 2.2). The UV–VIS/NIR spectrophotometer (Shimadzu, UV-2550) was used to gather all the required spectra. The average molecular weight (M_w) of the polymers was determined by SEC-VISC-RALS using a Viscotek 270 Dual Detector apparatus with PEO-19K as a reference in MeOH (flow rate, 0.20 mL/min). The SII TG/DTA 6200 was used to perform the TGA of both polymers under N_2 flow at a heating rate of 10 °C/min. A Si-DF40 cantilever was used in the dynamic mode of AFM (Nano Navi II; Seiko Instruments Inc., Tokyo) to detect the topology of the polymers. A VersaSTAT4 electrochemical workstation was used for the electrochemical measurements (AMETEK, Princeton Applied Research,

USA). Wide angle XRD was measured by using a RINT ULTIMA III device with Cu K_α radiation (λ= 1.54 Å), a generator voltage of 40 kV, and a current of 40 mA. The electrochemical/EC studies were conducted using a conventional three-electrode system, which included a 0.1 M TBAP + 0.01 M $AgNO_3$ reference electrode, a polymer-coated ITO WE, a Pt wire CE, and an Ag/Ag^+ electrode in acetonitrile as the electrolyte. CIE 1976 color diagram were calculated from color space mathematical modeling using Microsoft Excel[56].

Synthesis of L_{TPB}

4,4′-Bis[(4-bromophenyl)phenylamino]biphenyl (667 mg, 1.0 mmol); compound **3** (957 mg, 2.2 mmol); $Pd(PPh_3)_4$ (58 mg, 0.05 mmol, 5%); and K_2CO_3 (1.38 g, 10 mmol) were dissolved in anhydrous DMSO (50 mL) in the presence of N_2. The reaction mixture was warmed to 110°C for 24 h. After the reaction mixture had cooled to room temperature with stirring for 2 h, water (100 mL) was added to it. The substance was filtered out after it had settled and was rinsed with water many times before being cleaned with MeOH. By purifying the light green-yellow solid residue using column chromatography on neutral Al_2O_3 and eluting it with $CHCl_3$, a light green-yellow solid known as **L_{TPB}** (76.4 mg, 68% yield) was produced. The data are as follows: ^{1}H NMR (400MHz, $CDCl_3$) δ 8.79 (s, 4H), 8.73–8.75(m, 4H), 8.67 (d, 4H), 7.99 (d, 4H), 7.89 (td, 4H), 7.73 (d, 4H), 7.59 (d, 4H), 7.52 (d, 4H), 7.34–7.38 (m, 4H), 7.31 (t, 4H), 7.07(t,2H). ^{13}CNMR (100 MHz, $CDCl_3$): δ 156.38, 156.03, 149.88, 149.22,147.49, 146.62, 141.35, 136.98, 135.18, 134.31, 129.46, 127.90, 127.80, 127.53, 127.13, 124.76, 124.53, 124.07, 123.91, 123.31, 121.48, 118.72. ESI-MS: [$C_{78}H_{54}N_8$] = Calcd m/z = 1103.35, found m/z = 1103.46.

Preparation of polyFeL_{TPB}

For MSP synthesis, we applied the previously discussed methodology. In the presence of N_2, **L_{TPB}** (110.3 mg, 0.1 mmol) and $Fe(OAc)_2$ (17.93 mg, 0.1 mmol) were mixed and refluxed in 100% acetic acid for 24 h. After reaching room temperature, the reaction mixture was filtered to remove any insoluble residues. To eliminate acetic acid, the **polyFeL_{TPB}** solution was preserved in a Petri dish at room temperature. After vacuum drying, **polyFeL_{TPB}** was generated at an 88% yield.

Preparation of polyRuL_{TPB}

L_{TPB} (110.3 mg, 0.1 mmol) and $Ru(DMSO)_4Cl_2$ (44.8 mg, 0.1 mmol) were mixed in ethylene glycol and heated to reflux in an N_2-saturated environment for 24 h to create **polyRuL_{TPB}**. A vacuum pump was used to concentrate the reaction mixture, which was added dropwise to a cold tetrahydrofuran (THF) solution (100 mL) with stirring for 2 h. A slowly precipitating brown-red material was recovered by vacuum filtration, washed three to four times with THF, and treated with diethyl ether. To create **polyRuL_{TPB}** with a yield exceeding 87%, the polymer was dried for 24 h in a vacuum oven at 50°C.

Polymer film preparation on ITO

The polymer-coated ITO glass was prepared through a spin-coating technique. First, the polymers were dissolved (5 mg/mL) in dry methanol and 100 µL of the polymer solution was used for spin-coating on an ITO glass (2.5 × 2.5 cm^2) for 600 s at 120 rpm to prepare a polymer film with 150-200 nm thickness. The EC film was dried for 24 h at room temperature.

Counter electrode preparation

Spin-coating was performed on the ITO substrate for 30 s at 1000 rpm using a water-dispersed solution of nickel hexacyanoferrate (NiHCF). The film was exposed to an 85°C hotplate for 1 h before being left at room temperature for 24 h. For the CE in solid-state device manufacturing, the ITO glass coated with NiHCF was used.

Preparation of the semigel electrolyte

A mixture of acetonitrile (21 mL), lithium perchlorate (0.9 g), and propylene carbonate (6 mL) was poured into a 20-mL vial and stirred until it dissolved to create a very clear solution. PMMA (TCI, 2.1g) was gradually added after vigorous stirring. After 12 h, the matrix polymer had disintegrated. The viscous semigel liquid electrolyte was used in the construction of the ECD.

Solid-state device fabrication (ECD)

First, a NiHCF-coated ITO glass was covered by the transparent semigel electrolyte as a CE. The gel on ITO was kept for 2 h at room temperature. Surface treatment of the polymer-coated ITO film was conducted thrice before fabricating the ECD. The electrolyte gel was added to the polymer film and after 10 min, it was removed. The process was repeated thrice. Finally, the CE with gel electrolyte was placed over it and it was used for experiments. To maintain the cell gap between two electrodes we have placed a few silicon spheres with a diameter of 2.0 mm.

ASSOCIATED CONTENT

Supporting Information

The Supporting Information is available free of charge on the ACS Publications website. Material characterization, Comparison the ^{1}H-NMR spectra of $\mathbf{L_{TPB}}$ and polymers, Molecular weight measurement, TGA study, Scan rate-dependent CV study, integrating positive and negative current, comparing net charge of the polymers, UV–vis–NIR study of polymers and CIE chromaticity diagram of polymer films.

AUTHOR INFORMATION

Corresponding Author

Masayoshi Higuchi

Electronic Functional Macromolecules Group, Research Center for Functional Materials, National, Institute for Materials Science (NIMS), Tsukuba, Ibaraki 305- 0044, Japan.

Orcid ID: 0000-0001-9877-1134.

E-mail: HIGUCHI.Masayoshi@nims.go.jp

Authors

Dines Chandra Santra

Electronic Functional Macromolecules Group, National, Institute for Materials Science (NIMS), Tsukuba, Ibaraki 305- 0044, Japan.

Orcid ID: 0000-0002-9292-9524

Sanjoy Mondal

Electronic Functional Macromolecules Group, National, Institute for Materials Science (NIMS), Tsukuba, Ibaraki 305- 0044, Japan.

Present address: Sarat Centenary College, Dhaniakhali, Hooghly, West Bengal, India 712302

Orcid ID: 0000-0002-4391- 6356

Banchhanidhi Prusti

Electronic Functional Macromolecules Group, National, Institute for Materials Science (NIMS), Tsukuba, Ibaraki 305- 0044, Japan.

Orcid ID: 0000-0003-4489-2509

ACKNOWLEDGMENT

This research work was financially supported by the Mirai project (grant number: JPMJMI21I4) from the Japan Science and Technology Agency (JST) and the Environment Research and Technology Development Fund (ERTDF) (JPMEERF20221M02) from Environmental Restoration and Conservation Agency (ERCA).

REFERENCES

(1) Shehabi, A.; DeForest, N.; McNeil, A.; Masanet, E.; Greenblatt, J.; Lee, E. S.; Masson, G.; Helms, B. A.; Milliron, D. J. U.S. Energy Savings Potential from Dynamic Daylighting Control glazings. *Energy Build.* **2013,** 66, 415-423.

(2) Pérez-Lombard, L.; Ortiz, J.; Pout, C. A Review on Buildings Energy Consumption Information. *Energy Build.* **2008**, 40 (3), 394-398.

(3) Wen, R.-T.; Granqvist, C. G.; Niklasson, G. A. Eliminating Degradation and Uncovering Ion-Trapping Dynamics in Electrochromic WO3 Thin Films. *Nat. Mater.* **2015**, 14 (10), 996-1001.

(4) Wang, Z.; Wang, X.; Cong, S.; Geng, F.; Zhao, Z. Fusing electrochromic technology with other advanced technologies: A new roadmap for future development. *Mater. Sci. Eng.* **2020**, 140, 100524.

(5) Halder, S.; Roy, S.; Dixit, M.; Chakraborty, C. A Terpyridine Based Hydrogel System for Reversible Transmissive-to-Dark Electrochromism and Bright-to-Quenched Electrofluorochromism. *Chem. Commun.* **2022**, 58 (60), 8368-8371.

(6) De Forest, N.; Shehabi, A.; O'Donnell, J.; Garcia, G.; Greenblatt, J.; Lee, E. S.; Selkowitz, S.; Milliron, D. J. United States Energy and CO2 Savings Potential from Deployment of Near-Infrared Electrochromic Window Glazings. *Build. Environ.* **2015**, 89, 107-117.

(7) Granqvist, C.-G. Out of a niche. *Nat. Mater.* **2006**, 5 (2), 89-90.

(8) Grätzel, M. Ultrafast colour displays. *Nature* **2001**, 409 (6820), 575-576.

(9) Llordés, A.; Garcia, G.; Gazquez, J.; Milliron, D. J. Tunable Near-Infrared and Visible-Light Transmittance in Nanocrystal-in-Glass Composites. *Nature* **2013**, 500 (7462), 323-326.

(10) Chou, H. H.; Nguyen, A.; Chortos, A.; To, J. W.; Lu, C.; Mei, J.; Kurosawa, T.; Bae, W. G.; Tok, J. B.; Bao, Z. A Chameleon-Inspired Stretchable Electronic Skin with Interactive Colour Changing Controlled by Tactile Sensing. *Nat Commun*. **2015**, 6, 8011.

(11) Cai, G.; Wang, J.; Lee, P. S. Next-Generation Multifunctional Electrochromic Devices. *Acc. Chem. Res.* **2016**, 49 (8), 1469-1476.

(12) Mortimer, R. J. Electrochromic Materials. *Annu. Rev. Mater. Res.* **2011**, 41 (1), 241-268.

(13) Deb, S. K. Opportunities and Challenges in Science and Technology of WO3 for Electrochromic and Related Applications. *Sol. Energy Mater. Sol. Cells* **2008**, 92 (2), 245-258.

(14) Thakur, V. K.; Ding, G.; Ma, J.; Lee, P. S.; Lu, X. Hybrid Materials and Polymer Electrolytes for Electrochromic Device Applications. *Adv. Mater.* **2012**, 24 (30), 4071-4096.

(15) Zhong, Y.-W.; Yao, C.-J.; Nie, H.-J. Electropolymerized Films of Vinyl-Substituted Polypyridine Complexes: Synthesis, Characterization, and Applications. *Coord. Chem. Rev.* **2013**, 257 (7), 1357-1372.

(16) Madasamy, K.; Velayutham, D.; Suryanarayanan, V.; Kathiresan, M.; Ho, K.-C. Viologen-Based Electrochromic Materials and Devices. *J. Mater. Chem. C* **2019**, 7 (16), 4622-4637.

(17) Beaujuge, P. M.; Reynolds, J. R. Color Control in pi-Conjugated Organic Polymers for Use in Electrochromic Devices. *Chem. Rev.* **2010**, 110 (1), 268-320.

(18) Sarkar, M.; Dutta, T. K.; Patra, A. Two-dimensional Covalent Organic Frameworks for Electrochromic Switching. Chem. Asian. J 2021, 16 (20), 3055-3067.

(19) Bessinger, D.; Muggli, K.; Beetz, M.; Auras, F.; Bein, T. Fast-Switching Vis–IR Electrochromic Covalent Organic Frameworks. *J. Am. Chem. Soc.* **2021**, 143 (19), 7351-7357.

(20) Hao, Q.; Li, Z.-J.; Bai, B.; Zhang, X.; Zhong, Y.-W.; Wan, L.-J.; Wang, D. A Covalent Organic Framework Film for Three-State Near-Infrared Electrochromism and a Molecular Logic Gate. *Angew. Chem. In. Ed.* **2021**, 60 (22), 12498-12503.

(21) Wang, G.; Fu, X.; Huang, J.; Wu, C.; Wu, L.; Du, Q. Synthesis of a New Star-Shaped 4,4′ -Bipyridine Derivative and its Multicolor Solid Electrochromic Devices. *Org. Electron.* **2011**, 12 (7), 1216-1222.

(22) Alesanco, Y.; Viñuales, A.; Palenzuela, J.; Odriozola, I.; Cabañero, G.; Rodriguez, J.; Tena-Zaera, R. Multicolor Electrochromics: Rainbow-Like Devices. *ACS Appl. Mater. Interfaces.* **2016**, 8 (23), 14795-14801.

(23) Rao, T.; Zhou, Y.; Jiang, J.; Yang, P.; Liao, W. Low Dimensional Transition Metal Oxide Towards Advanced Electrochromic Devices. *Nano Energy* **2022**, 100, 107479.

(24) Wu, W.; Wang, M.; Ma, J.; Cao, Y.; Deng, Y. Electrochromic Metal Oxides: Recent Progress and Prospect. *Adv. Electron. Mater*. **2018**, 4 (8), 1800185.

(25) Fan, H.; Wei, W.; Hou, C.; Zhang, Q.; Li, Y.; Li, K.; Wang, H. Wearable Electrochromic Materials and Devices: FromVisible to Infrared Modulation. *J. Mater.Chem. C* **2023**, 11 (22), 7183-7210.

(26) Wei, H.; Yan, X.; Wu, S.; Luo, Z.; Wei, S.; Guo, Z. Electropolymerized Polyaniline Stabilized Tungsten Oxide Nanocomposite Films: Electrochromic Behavior and Electrochemical Energy Storage. *J. Phys. Chem. C* **2012**, 116 (47), 25052-25064.

(27) Nguyen, T. V.; Le, Q. V.; Peng, S.; Dai, Z.; Ahn, S. H.; Kim, S. Y. Exploring Conducting Polymers as a Promising Alternative for Electrochromic Devices. *Adv. Mater. Technol.* **2023**, 8 (18), 2300474.

(28) Kim, J.; In, Y. R.; Phan, T. N.-L.; Kim, Y. M.; Ha, J.-W.; Yoon, S. C.; Kim, B. J.; Moon, H. C. Design of Dithienopyran-Based Conjugated Polymers for High-Performance Electrochromic Devices. *Chem. Mater.* **2023**, 35 (2), 792-800.

(29) Cannavale, A.; Cossari, P.; Eperon, G. E.; Colella, S.; Fiorito, F.; Gigli, G.; Snaith, H. J.; Listorti, A. Forthcoming Perspectives of Photoelectrochromic Devices: A Critical Review. *Energy Environ Sci.* **2016**, 9 (9), 2682-2719.

(30) Khandelwal, H.; Schenning, A. P. H. J.; Debije, M. G. Infrared Regulating Smart Window Based on Organic Materials. *Adv. Energy Mater.* **2017**, 7 (14), 1602209.

(31) Granqvist, C. G. Oxide Electrochromics: An Introduction to Devices and Materials. *Sol Energy Mater. Sol. Cells* **2012**, 99, 1-13.

(32) Lee, S.-H.; Deshpande, R.; Parilla, P. A.; Jones, K. M.; To, B.; Mahan, A. H.; Dillon, A. C. Crystalline WO3 Nanoparticles for Highly Improved Electrochromic Applications. *Adv. Mater*. **2006**, 18 (6), 763-766.

(33) Howard, E. L.; Österholm, A. M.; Shen, D. E.; Panchumarti, L. P.; Pinheiro, C.; Reynolds, J. R. Cost-Effective, Flexible, and Colorful Dynamic Displays: Removing Underlying Conducting Layers from Polymer-Based Electrochromic Devices. *ACS Appl. Mater. Interfaces,* **2021**, 13 (14), 16732-16743.

(34) Christiansen, D. T.; Ohtani, S.; Chujo, Y.; Tomlinson, A. L.; Reynolds, J. R. All Donor Electrochromic Polymers Tunable across the Visible Spectrum via Random Copolymerization. *Chem. Mater.* **2019**, 31 (17), 6841-6849.

(35) Lo, C. K.; Shen, D. E.; Reynolds, J. R. Fine-Tuning the Color Hue of π-Conjugated Black-to-Clear Electrochromic Random Copolymers. *Macromolecules* **2019**, 52 (17), 6773-6779.

(36) Santra, D. C.; Nad, S.; Malik, S. Electrochemical Polymerization of Triphenylamine End-Capped Dendron: Electrochromic and Eectrofluorochromic Switching Behaviors. *J. Electroanalytical Chem.* **2018**, 823, 203-212.

(37) Bera, M. K.; Ninomiya, Y.; Higuchi, M. Constructing Alternated Heterobimetallic [Fe(II)/Os(II)] Supramolecular Polymers with Diverse Solubility for Facile Fabrication of Voltage-Tunable Multicolor Electrochromic Devices. *ACS Appl. Mater. Interfaces.* **2020**, 12 (12), 14376-14385.

(38) Bera, M. K.; Ninomiya, Y.; Higuchi, M. Stepwise Introduction of Three Different Transition Metals in Metallo-Supramolecular Polymer for Quad-Color Electrochromism. *Commun. Chem*. **2021**, 4 (1), 56.

(39) Santra, D. C.; Mondal, S.; Yoshida, T.; Ninomiya, Y.; Higuchi, M. Ru(II)-Based Metallo-Supramolecular Polymer with Tetrakis(N-methylbenzimidazolyl)bipyridine for a Durable, Nonvolatile, and Electrochromic Device Driven at 0.6 V. *ACS Appl. Mater. Interfaces* **2021**, 13 (26), 31153-31162.

(40) Puodziukynaite, E.; Oberst, J. L.; Dyer, A. L.; Reynolds, J. R. Establishing Dual Electrogenerated Chemiluminescence and Multicolor Electrochromism in Functional Ionic Transition-Metal Complexes. *J. Am. Chem. Soc.* **2012**, 134 (2), 968-978.

(41) Zhong, Y.-W.; Yao, C.-J.; Nie, H.-J. Electropolymerized Films of Vinyl-Substituted Polypyridine Complexes: Synthesis,Characterization, and Applications. *Coord. Chem. Rev*. **2013**, 257 (7), 1357-1372.

(42) Bera, M. K.; Ninomiya, Y.; Higuchi, M. Constructing Alternated Heterobimetallic [Fe(II)/Os(II)] Supramolecular Polymers with Diverse Solubility for Facile Fabrication of Voltage-Tunable Multicolor Electrochromic Devices. *ACS Appl. Mater. Interfaces,* **2020,** 12 (12), 14376-14385.

(43) Kim, J.; Ong, G. K.; Wang, Y.; LeBlanc, G.; Williams, T. E.; Mattox, T. M.; Helms, B. A.; Milliron, D. J. Nanocomposite Architecture for Rapid, Spectrally-Selective Electrochromic Modulation of Solar Transmittance. *Nano Lett.* **2015**, 15 (8), 5574-5579.

(44) Brooke, R.; Mitraka, E.; Sardar, S.; Sandberg, M.; Sawatdee, A.; Berggren, M.; Crispin, X.; Jonsson, M. P. Infrared Electrochromic Conducting Polymer Devices. *J Mater. Chem. C* **2017**, 5 (23), 5824-5830.

(45) Lin, L.-C.; Yen, H.-J.; Kung, Y.-R.; Leu, C.-M.; Lee, T.-M.; Liou, G.-S. Novel Near-Infrared and Multi-Colored Electrochromic Polybenzoxazines with Electroactive Triarylamine moieties. *J. Mater. Chem. C* **2014**, 2 (37), 7796-7803.

(46) Chakraborty, C.; Rana, U.; S. L. V. Narayana, Y.; Moriyama, S.; Higuchi, M. Helical Fe(II)-Based Metallo-Supramolecular Polymers: Effect of Crown Ether Groups Located outside the Helix on Hydrous Proton Channel Formation. *ACS Appl. Poly. Mater.* **2020**, 2 (11), 4521-4530.

(47) Mondal, S.; Chandra Santra, D.; Ninomiya, Y.; Yoshida, T.; Higuchi, M. Dual-Redox System of Metallo-Supramolecular Polymers for Visible-to-Near-IR Modulable Electrochromism and Durable Device Fabrication. *ACS Appl. Mater. Interfaces* **2020**, 12 (52), 58277-58286.

(48) Yang, X.; Zhang, Y.; Zhang, B.; Zhang, S.; Liu, X.; Li, G.; Chu, D.; Zhao, Y.; He, G. Electron-Accepting Carborane Viologen and Iron Based-Supramolecular Polymers for Electrochromism and Enhanced Photocatalytic Hydrogen Evolution. *J. Mater. Chem. C* **2020**, 8 (46), 16326-16332.

(49) Yen, H.-J.; Lin, K.-Y.; Liou, G.-S. Transmissive to Black Electrochromic Aramids with High Near-Infrared and Multicolor Electrochromism Based on Electroactive Tetraphenylbenzidine Units. *J. Materi. Chem.* **2011**, 21 (17), 6230-6237.

(50) Lv, X.; Li, J.; Xu, L.; Zhu, X.; Tameev, A.; Nekrasov, A.; Kim, G.; Xu, H.; Zhang, C. Colorless to Multicolored, Fast Switching, and Highly Stable Electrochromic Devices Based on Thermally Cross-Linking Copolymer. *ACS Appl. Mater. Interfaces* **2021**, 13 (35), 41826-41835.

(51) Dhanker, R.; Gray, C. L.; Mukhopadhyay, S.; Nunez, S.; Cheng, C.-Y.; Sokolov, A. N.; Giebink, N. C. Large Bipolaron Density at Organic Semiconductor/Electrode Interfaces. *Nat. Commun.* **2017**, 8 (1), 2252.

(52) Chandra Santra, D.; Mondal, S.; Malik, S. Design of Triphenylamine Appended Anthracene Derivatives: Electro-Polymerization and Their Electro-Chromic Behaviour. *RSC Adv.* **2016**, 6 (85), 81597-81606.

(53) Zheng, S.; Barlow, S.; Risko, C.; Kinnibrugh, T. L.; Khrustalev, V. N.; Jones, S. C.; Antipin, M. Y.; Tucker, N. M.; Timofeeva, T. V.; Coropceanu, V.; et al. Isolation and Crystal Structures of Two Singlet Bis(Triarylamine) Dications with Nonquinoidal Geometries. *J. Am. Chem. Soc.* **2006**, 128 (6), 1812-1817. DOI: 10.1021/ja0541534.

(54) Huang, C.-L.; Kung, Y.-R.; Shao, Y.-J.; Liou, G.-S. Synthesis and Characteristics of Novel TPA-Containing Electrochromic Poly(ether sulfone)s with Dimethylamino Substituents. *Electrochim. Acta* **2021**, 368, 137552.

(55) Roy, M.; Walton, J. H.; Fettinger, J. C.; Balch, A. L. Direct Crystallization of Diamine Radical Cations: Carbon-Nitrogen Bond Formation from the Reaction of

Triphenylamine with TiCl4, TiBr4, or SnCl4 versus Carbon-Carbon Bond Formation with SbCl5**. *Chem.Euro. J.* **2022**, 28 (17), e202104631.

(56) Yen, H.-J.; Liou, G.-S. Solution-Processable Novel Near-Infrared Electrochromic Aromatic Polyamides Based on Electroactive Tetraphenyl-p-Phenylenediamine Moieties. *Chem. Mater.* **2009**, 21 (17), 4062-4070.

(57) Yen, H.-J.; Lin, K.-Y.; Liou, G.-S. Transmissive to black electrochromic aramids with high near-infrared and multicolor electrochromism based on electroactive tetraphenylbenzidine units. *J. Mater. Chem. C* **2011**, 21 (17), 6230-6237, 10.1039/C1JM10210A.

(58) Robin, M. B.; Day, P. Mixed Valence Chemistry-A Survey and Classification. In Adv. Inorg. Radiochem., Emeléus, H. J., Sharpe, A. G. Eds.; Vol. 10; Academic Press, 1968; pp 247-422.

(59) Feng, J.; Shao, J.-Y.; Nie, H.-J.; Gong, Z.-L.; Zhong, Y.-W. Synthesis and electrochemical and spectroscopic studies of a N,N,N',N'-tetraphenylbenzidine-bridged bis(2,2'-bipyridine) ligand and diruthenium complex. *Chinese Chem. Lett.* **2018**, 29 (3), 385-389.

(60) Delgado-González, M. J.; Carmona-Jiménez, Y.; Rodríguez-Dodero, M. C.; García-Moreno, M. V. Color Space Mathematical Modeling Using Microsoft Excel. J. *Chem.Educ.* **2018**, 95 (10), 1885-1889.

(61) Lu, H.-C.; Hsiao, L.-Y.; Kao, S.-Y.; Seino, Y.; Santra, D. C.; Ho, K.-C.; Higuchi, M. Durable Electrochromic Devices Driven at 0.8 V by Complementary Chromic Combination of Metallo-Supramolecular Polymer and Prussian Blue Analogues for

Smart Windows with Low-Energy Consumption. *ACS Appl. Electron. Mater.* **2021**, 3 (5), 2123-2135.

(62) Mondal, S.; Yoshida, T.; Maji, S.; Ariga, K.; Higuchi, M. Transparent Supercapacitor Display with Redox-Active Metallo-Supramolecular Polymer Films. *ACS Appl. Mater. Interfaces* **2020**, 12 (14), 16342-16349.

(63) Macher, S.; Rumpel, M.; Schott, M.; Posset, U.; Giffin, G. A.; Löbmann, P. Avoiding Voltage-Induced Degradation in PET-ITO-Based Flexible Electrochromic Devices. *ACS Appl. Mater. Interfaces* **2020,** 12 (32), 36695-36705.

TOC